

Experimental and Numerical Studies on Tensile and Shear Fracturing of Brittle Materials

Nazife ERARSLAN^{*1}

¹Adana Bilim ve Teknoloji Üniversitesi, Mühendislik ve Doğa Bilimleri Fakültesi,
Maden ve Cevher Hazırlama Mühendisliği, Adana

Geliş tarihi: 13.04.2017

Kabul tarihi: 31.05.2017

Abstract

Sudden and violent fracturing of brittle materials, such as rocks and concretes, still remain one of the leading causes of fatalities in mining, civil and geotechnical industries today. The primary aim of this study is to investigate the mixed modes, mode I (tensile) and mode II (shearing) fracturing mechanisms of rock and prepared concrete specimens using Crack Chevron Notched Brazillian Disc (CCNBD) specimen geometries. Static diametrical compression tests showed that the notched cracks at the centre of the specimens opened (Mode I) up to 30° crack inclination angle (β), whereas crack closure started for $\beta > 33^\circ$, and closure became more pronounced at even higher β of 45° and 70°. A series of numerical analyses were then performed by using a Finite Element Method (FEM) software FRANC2D to simulate the stress distributions and fracturing behaviour of the samples at different β , and to obtain the Mode I and Mode II fracture toughness values K_{Ic} and K_{IIc} respectively. According to the numerical results, it was unlikely to obtain pure Modes I and II using both the CCNBD specimens under diametral compressive loading. Furthermore, the numerical simulations also suggested that K_{Ic} was more effective on crack initiation than K_{IIc} ; whereas, at the onset of crack propagation, the opposite was the case.

Keywords: Fracture toughness, Mode I and Mode II fracturing, FRANC2D, Fracturing of rock and concrete

Kırılgan Malzemelerin Çekme ve Makaslama Kırılmaları Üzerinde Deneysel ve Sayısal Çalışmalar

Öz

Kayalar ve beton gibi kırılgan malzemelerin ani ve şiddetli kırılmaları hala madencilik ve inşaat endüstrilerinde ölümcül olayların sebepleridir. Bu çalışmanın temel amacı ortak kırılma modu olan modeI-II, mod I (çekme kırılmaları) ve mod II (makaslama) kırılmalarından oluşan yenilmelerin, hazırlanmış CCNBD ismi verilen kaya ve beton numuneler ile incelenmesidir. Statik çapsal basma gerilmesi altında test edilen numunelerde, çatlak eğim açısı β , 30° olana kadar çentik çatlağında Mod I kırılmaya neden olan açılmalar görülmüştür. Bunun yanında β açısı 33°den büyük olduğunda ise çentik çatlağında kapanma gözlenmiştir ve bu kapanma β açısı 45° ve 70° olduğunda oldukça fazla ve belirgin olmuştur. Sonlu elemanlar yöntemi ile işleyen FRANC2D programı kullanarak sayısal modellemeler

* Sorumlu yazar (Corresponding author): Nazife ERARSLAN, nerarслан@adanabtu.edu.tr

yapılmıştır ve gerilme dağılımı analizi, çatlaklanma modelleri yapılarak Mod I ve II tıkızlık değerleri olan K_{Ic} and K_{IIc} değerleri bulunmuştur. Sayısal analiz sonuçlarına göre, çapsal basma gerilmesi altında test edilen CCNBD numunelerde salt Mod I veya salt Mod II kırılmaların mümkün olmadığı bulunmuştur. Ayrıca sayısal analiz sonuçları, çatlaklanmanın başlamasında mode I tıkızlık değeri olan K_{Ic} 'nin Mod II tıkızlık değeri K_{IIc} 'den daha baskın olduğu ve oluşmuş çatlağın ilerlemesinde ise tam tersi olduğunu göstermiştir.

Anahtar Kelimeler: Kırılma tıkızlığı, Mod I ve Mod II kırılma, FRANC2D, Kaya ve beton kırılmaları

1. INTRODUCTION

Rapid and violent failures of large-scale mining or civil engineering rock structures can cause significant safety hazards, material damage and interruption to mining or building activities. The fundamental questions in both mining and civil engineering relate to predicting the failure load of rock structures consisting of flaws and cracks, and to revealing the combination of load and flaw geometry that lead to failure. Rock fracture mechanics is one approach to recognising pre-failure rock mass behaviour, which may result in predicting or preventing the potential for geotechnical and geological failure [1]. Fracture mechanics, sometimes called crack mechanics, is concerned with the individual crack or cracks. Moreover, existing failure criteria and theories, such as the well-known Coulomb Criterion, often deal directly with fracture processes; however, they cannot be expected to deal with crack propagation in terms of the length of the crack or the direction of crack propagation. Fracture mechanics or, more specifically, linear elastic fracture mechanics (LEFM), has become well developed over the past 50 years, as engineers tried to understand the brittle failure of structures made of high-strength metal alloys [2]. However, fracture mechanics was only applied to the study of rock fracturing in the 1980s [3]. Some past research on rock and concrete fracture mechanics has provided significant knowledge on tensile fracturing (Mode I fracturing) [4, 5].

Cracks or discontinuities in brittle materials such as rocks and concrete are not subjected to just one type of loading. Some rock structures, such as bridge abutments, dam and road foundations, and tunnel walls, undergo both static and cyclic

loading caused by, for example, vehicle-induced vibrations, drilling and blasting or traffic. This type of loading often causes rock to fail at a lower than expected stress. The design of such structures requires understanding of, and research on, rock mechanical parameters under various loading conditions. LEFM is based on the stress intensity factor (SIF), K , which quantifies the intensity of the stress singularity at the crack tip. Fracture mechanics states that a crack will propagate when its stress intensity reaches a critical value, K_{Ic} , assuming that the crack tip is in a state of plane strain. The stress intensity factor depends on the fracture displacement modes and crack geometry.

A crack can deform in three basic modes: Mode I, Mode II and Mode III. The classification of fracturing is based on the crack surface displacement or the crack tip loading [3, 7]. Mode I, which is also called the opening (tensile) mode, is so called because the crack tip is subjected to a normal stress and the crack faces separate symmetrically with respect to the crack front, so that the displacements of the crack surfaces are perpendicular to the crack plane (Figure 1). The crack carries no shear traction and no shear displacement is visible. Mode II is the edge sliding (or in-plane shearing) mode, where the crack tip is subjected to an in-plane shear stress and the crack faces slide relative to each other so that the displacements of the crack surfaces are in the crack plane and are perpendicular to the crack front (Figure 1). Mode III is the tearing mode, as the crack tip is subjected to an out-of-plane shear stress. The crack faces move relative to each other so that the displacements of the crack surfaces are in the crack plane but are parallel to the crack front (Figure 1) [8, 9].

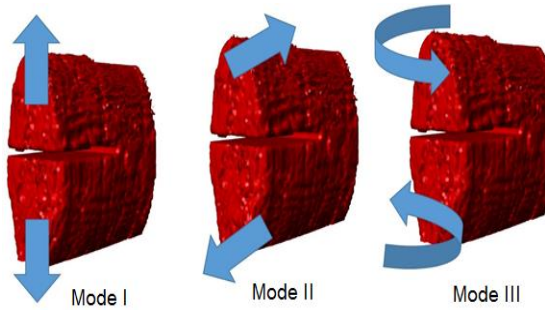


Figure 1.Fracturing modes of brittle materials [10]

Stress Intensity Factor (SIF) and maximum SIF, K_{Ic} , the widely accepted LEFM model today which describes the stress field in the area at the crack tip can be obtained in Equation 1 [11].

$$K_{Ic} = \sigma \sqrt{\pi a} \quad (1)$$

Where, K_{Ic} , critical SIF as a measure of material resistance to fracture which is also known as the fracture toughness, σ is applied stress and a is length of the crack.

Mixed mode I–II fracture problems under compressive loading are shown to be more complicated than, and also quite different from, those under tension. In general, it is accepted that tensile cracks grow initially at an angle with respect to the direction of the compressive stress, and then rapidly grow in the direction of the compressive stress [12, 13, 14]. The fracture stresses for Mode I, Mode II and mixed Mode I–II compressive loading can be found similarly to those for tension loading by using the three fracture criteria used in fracture mechanics [15]. In contrast, some researchers have provided a closed-form solution for the stress distribution in cracked and uncracked disc specimens under diametral compression [4, 5, 16]. Shetty et al. [5] first used a CSNBD specimen to calculate both Mode I and Mode II fracture toughnesses of ceramics. Atkinson [4], Awaji and Sato [16] developed dimensionless Mode I stress intensity factor (NI) and dimensionless Mode II stress intensity factor (NII) solutions depending on the dimensionless notch length α (a/R) and the notch inclination angle (β) with respect to the loading direction.

Generalised Maximum Tangential Stress (GMTS) criterion is used in general to describe and calculate the tangential stress in front of the crack tip under mixed Mode I–II loading [18]. The GMTS criterion has been specifically modified for the SCB geometry samples to model its crack propagation under mixed-Mode I–II loading as given in Equations 2 and 3 [18].

$$K_{Ic} = \frac{P\sqrt{\pi a}}{2Rt} Y_I \left(\alpha, \frac{a}{R}, \frac{S}{R} \right) \quad (2)$$

$$K_{IIc} = \frac{P\sqrt{\pi a}}{2Rt} Y_{II} \left(\alpha, \frac{a}{R}, \frac{S}{R} \right) \quad (3)$$

Where, K_{Ic} , K_{IIc} dimensional Mode I and Mode II SIFs respectively, P is compressive applied loading, a is length of the crack, t is thickness of the specimen, R is radius of the specimen, Y_I and Y_{II} are Mode I and Mode II geometry factors respectively.

2. TESTING METHODOLOGY AND EXPERIMENTAL RESULTS

2.1. Geometry of the Specimens

The geometry of a CCNBD specimen is illustrated in Figure 2. The thickness of the notches, t , was 1.5 mm and the thickness of the specimens, B , was 25 mm. The inner chevron notched crack length, $2a_0$, was 16–18 mm and the outer chevron notched crack length, $2a_1$, was 36–37 mm. All geometrical dimensions should be converted to dimensionless parameters with respect to the specimen radius and diameter. Specimen dimensions are given in the suggested ISRM methods [20]. Other specimen geometrical dimensions are possible; however, in order to have a valid test, the two most important dimensions, that is, the dimensionless final notched crack length (α_1) and the dimensionless quantity (α_B), must fall within the range outlined in the suggested ISRM methods [20]. The dimensionless initial crack length ($\alpha_0 = a_0/R$), the dimensionless final notched crack length ($\alpha_1 = a_1/R$) and the dimensionless quantity ($\alpha_B = B/R$) are the three basic dimensions for the CCNBD specimens (Figure 2). All specimen geometries used in this

study were in the valid ranges suggested by the ISRM [20].

Disk specimens were diametrically loaded with various angles (β) inclined according to diametral compressive loading directions ranging from 0° to 70° . A load-controlled testing manner was adopted and loading was continued till failure. Load, diametral displacement and Crack Mouth Displacement (CMOD) were continually recorded during the test using a computerised data logger.

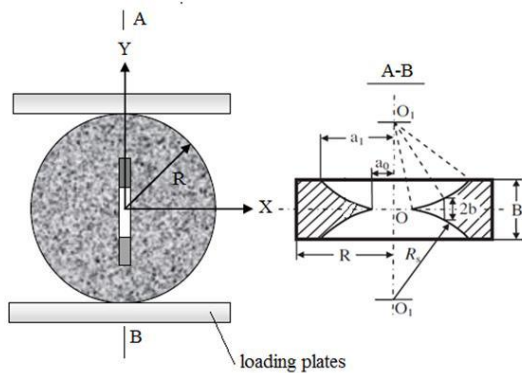


Figure 2. CCNBD specimen geometry with recommended test fixture

The failure load for both rock and concrete specimens were obtained from the fracture toughness tests and the results are summarised in Table 1.

Table 1. Failure load of rock and concrete specimens [9]

Geometry	Material type	Crack inclination angle, β ($^\circ$)	Failure Load (kN)
CCNBD	Concrete	0	4.82
		30	4.75
		45	4.94
		70	4.18
	Rock	0	5.498
		30	5.483
		45	5.969
		70	6.217

In general, failure load increases with increasing β for all rock and concrete specimens. The results show that diametral compressive loading along the crack plane in CCNBD specimens always creates mixed-mode fracturing, without any clear Mode II fracturing, although the crack is subjected to compressive-shear loading.

Table 2. Theoretical fracture toughness results [9]

Material	Crack Inclination Angle β ($^\circ$)	Theoretical Fracture Toughness Results ($\text{Mpa}\sqrt{\text{m}}$)	
		K_{Ic}	K_{IIc}
Concrete	0	0.3924	NA
	30	0.3241	0.6250
	45	0.3355	0.6470
	70	0.2896	0.5880
Brisbane Tuff Rock	0	0.8255	N/A
	30	0.8995	1.650
	45	1.028	1.857
	70	1.056	1.906

The tested rock and concrete specimens are shown in Figure 3. The crack initiation angle was found to be strongly dependent on the crack inclination angle (β) in experimental studies. It was found that cracks initiated at an angle of $70\text{--}100^\circ$ relative to the original crack plane when the inclined crack was subjected to uniaxial compressive stress. From the experimental results, cracks initiated at the tip of the notch for all three kind of rock specimens with values of β up to 30° only. However, one of the most important observations from the experimental findings was that the location of crack initiation moved to the centre of the notch crack with increasing crack inclination angle after 30° ($\beta \geq 30^\circ$). Also, it was found with 70° inclined cracks in rock samples that single coplanar shear cracks took place individually at one end of the tip of the cracks.

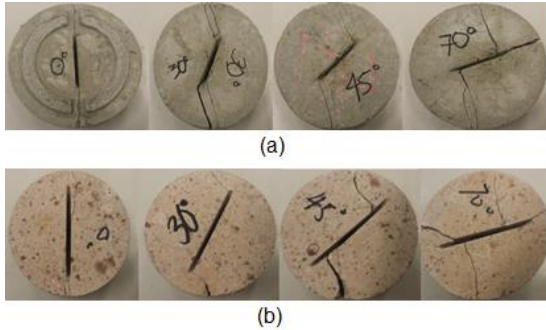


Figure 3. Tested CCNBD specimens (a) concrete and (b) rock specimens [9]

3. NUMERICAL ANALYSES AND RESULTS

A series of finite element simulations were conducted to model notched crack initiation and propagation under static diametral loading. The stress distribution and crack propagation analysis of the specimens were conducted using the finite element program FRANC2D (FRacture ANalysis Code). FRANC2D was originally developed at Cornell University and was accepted as a step in developing discrete fracture analysis programs [19]. The numerical model was built on the geometry of a Crack Straight Through Brazilian Disc (CSTBD) specimen, for which the parameters were diameter, $D = 52$ mm; thickness, $B = 25$ mm and notched crack length = 18 mm. All of the elements used in the finite element models have elastic–isotropic material parameters that were defined using the results obtained from the rock characterisation tests. The diametral compressive loads used in the numerical models were based on the ultimate loads obtained experimentally for various individual crack inclination angles. The bottom of the specimen disc was fixed in both x and y directions. The problem type was plain stress and the crack propagation was conducted using the ‘automatic non-cohesive crack propagation’ option of FRANC2D, since the cohesive crack model implemented in FRANC2D is for Mode I fracturing only. Hence, non-cohesive crack propagation was used to more accurately simulate the inclined crack propagation.

The first numerical modelling series was done for stress distribution analysis around a notch crack in a CCNBD specimen. The loading situations for various inclination angles were simulated properly without any new crack initiation or propagation to eliminate use of the mixed-mode fracture criterion (Figure 4). In general, the region of tensile stress distribution extends closer to the centre of the chevron notch crack with increasing crack inclination angles. The maximum tensile stress was obtained along the crack plane at the tip of the $\beta = 0^\circ$ inclined chevron notch.

In contrast, the maximum shear stress was found just under the loading boundary where the high compressive region occurred and the region of shear stress moved from the side of the end of the notch crack to the centre of the end of the notch crack after 30° crack inclination angle. The maximum tensile stresses were obtained at the tip of the notch crack in normal direction to the crack plane with $\beta = 28^\circ$, $\beta = 30^\circ$ and $\beta = 33^\circ$ inclined notch cracks.

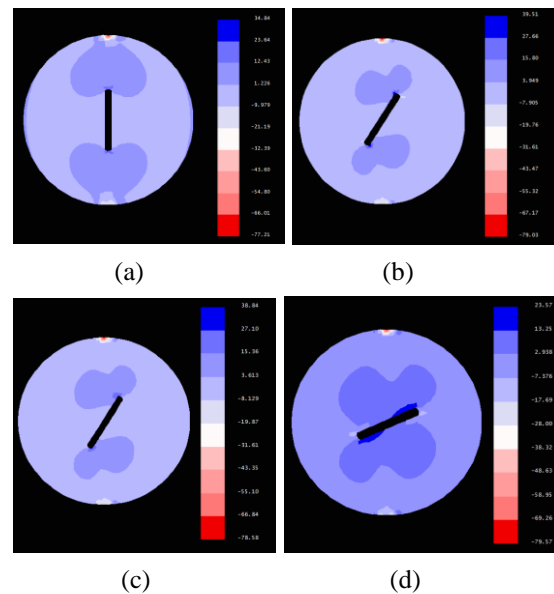


Figure 4. Stress distribution around the notch crack inclined at; (a) $\beta = 0^\circ$ (b) $\beta = 30^\circ$ (c) $\beta = 45^\circ$ and (d) $\beta = 70^\circ$

In general, the results of the numerical stress distribution analyses show that it is not possible to obtain pure mode I and pure mode II fracturing modes with uniform diametral compressive loading on to the CCNBD geometry. It was found that both normal stress (tension) and shear stress are effective with all inclination angles. Further, normal stress (tension) values are higher than the tensile strength of the material. Thus, it is hard to determine which fracturing mode acts in crack propagation first.

In addition to the contour plots for stress distribution, the ‘line plot’ postprocess option of FRANC2D is used to analyse stress distribution around the notch crack in detail. We named the position at the left-hand side of the notch crack the ‘upper face of crack’ and at the right-hand side the ‘lower face of crack’ according to the diametral compressive loading and inclination of the notch crack (Figure 5). The upper end of the line represents the start point of the ‘position on line’ axis in the plots (Figure 5).

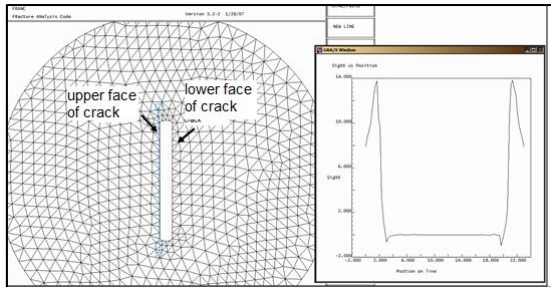


Figure 5. Line plot post-process option of FRANC2D for stress distribution analysis around notch crack

Stress distribution around the tip of a notch crack best can be explained by plotting the normal stress, shear stress, and stress in the x-axis separately along the upper face, lower face and at the tip of the notch crack. Figure 5 shows the normal stress distribution around the upper face of a notch crack inclined at various inclination angles (β). The normal stress is tensile at the upper face of a notch crack inclined up to $\beta = 33^\circ$. In contrast, normal stress is compressive at the upper face of a notch

crack with inclination angles $\beta = 45^\circ$ and $\beta = 70^\circ$ (Figure 6). Figure 7 shows the normal stress distribution around the lower face of a notch crack with symmetrical results to those of the upper face. These results show points where wing crack initiations take place around the tip of the notch crack. However, normal stress is always compressive around both the lower and upper faces of a notch crack with inclination angles $\beta = 45^\circ$ and $\beta = 70^\circ$ (Figure 5 and Figure 7).

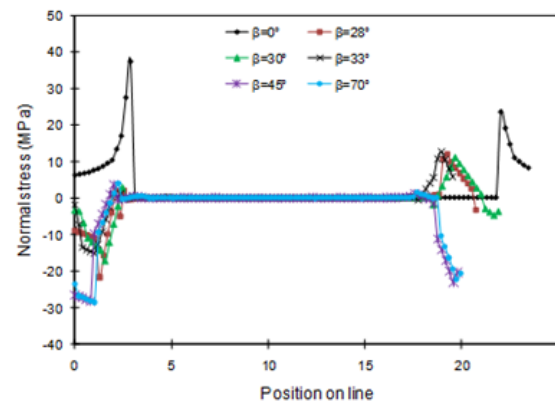


Figure 6. Normal stress (σ_n) distribution around the upper face of a notch crack (Tensile:+; Compressive:-)

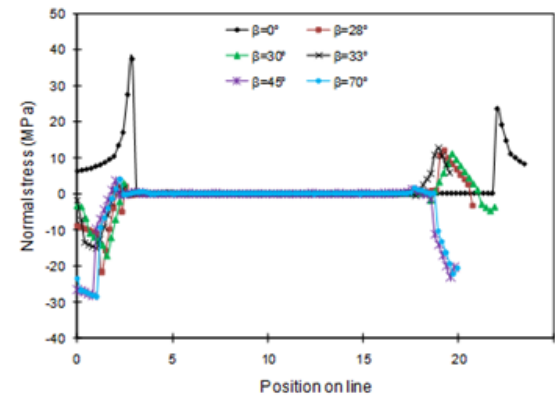


Figure 7. Normal stress (σ_n) distribution around the lower face of a notch crack (Tensile:+; Compressive:-)

After the stress distribution analysis, crack propagation analyses were done to investigate the

crack displacements depending on the crack inclination angles. FRANC2D was accepted as a step in developing the discrete fracture analysis programs. During performance of a discrete crack analysis for crack growth, not only the geometry of the crack is represented explicitly at each step, but also the mesh must be modified at each step to reflect the current crack configuration. The automatic re-meshing strategy adopted in FRANC2D is to delete the elements in the vicinity of the crack tip, move the crack tip, and then insert a trial mesh to connect the new crack to the existing mesh.

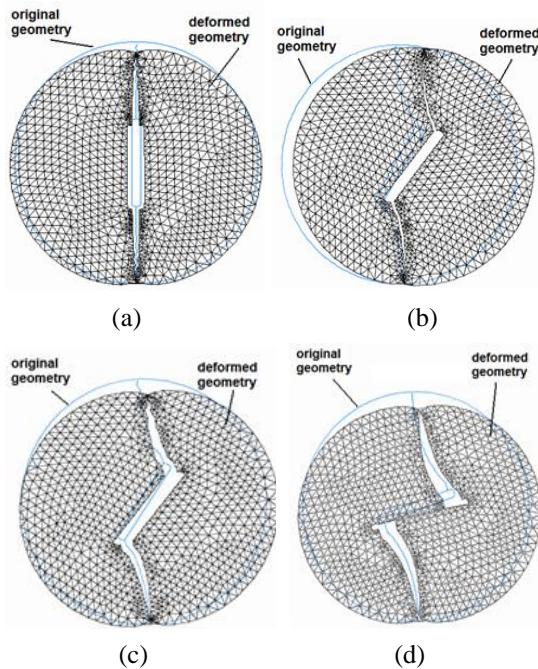


Figure 8. Simulated original and deformed notch cracks with various inclination angles (a) $\beta = 0^\circ$ (b) $\beta = 30^\circ$ (c) $\beta = 45^\circ$ and (d) $\beta = 70^\circ$

The crack propagation simulation results are shown in Figure 8. It was found that crack initiation angle was strongly dependent on the notch crack inclination angle. Moreover, the direction of crack propagation was found to be parallel to the loading direction and is in good agreement with experimental findings. Because the high tensile stress zone was observed to extend

along the centre of the notch crack instead of the tip of the notch crack with increasing inclination angle in the stress distribution analysis in the previous section, crack initiation in crack simulations starts from a region closer to the centre of the notch crack when the β increases.

4. CONCLUSIONS

Static loading tests performed on diametrically loaded CCNBD specimens showed that cracks initiated only at the tip of the notched crack when the inclination angle had a value of up to 30° . However, when the inclination angle was greater than 33° , the crack initiation point moved from the tip to the centre of the notched crack as the inclination angles increased. Moreover, it was found that all notched cracks opened for crack inclination angles (β) of up to 30° , whereas crack closing was found to start above that angle. The maximum crack closure was observed at a crack inclination of 70° for all rock and concrete samples. The amount of this closure is around 0.02 mm, which is much less than the width of the notch (2 mm). This means that the notch crack surface planes do not come in contact with each other before failure. In contrast, the maximum crack opening was observed at a crack inclination of 0° for all samples. It is clear that a diametral compressive loading along the crack plane in CCNBD samples always creates mixed-mode fracturing without any clear mode II fracturing, although the crack is subjected to the compressive-shear loading. Another important observation obtained from the load-CMOD graphs is the presence of plastic deformation regions before the peak load points. Because clear plastic deformation took place before failure in all rock and concrete samples, there is a possible Fracture Process Zone (FPZ) in front of the crack tip.

In order to check the validity of the numerical modelling, a comparison of numerical results and experimental findings regarding crack initiation and crack inclination (β) angles was made. A good agreement was found between numerical and experimental findings regarding crack extension (θ) and β . In general, the results of the numerical stress distribution analyses show that it is not

possible to obtain pure mode I and pure mode II fracturing modes with uniform diametral compressive loading on to the CCNBD geometry. It was found that both normal stress (tension) and shear stress are effective with all inclination angles. Further, normal stress (tension) values are higher than the tensile strength of the material. Thus, it is hard to determine which fracturing mode acts in crack propagation first. The crack initiation angle was found to increase with increasing crack inclination angles with the numerical results.

5. ACKNOWLEDGEMENTS

The corresponding author was supported by Adana Science and Technology University, Scientific Research Projects (BAP in TR) Coordination (Project No: MÜHDBF.MCHM.2015-17) and The Scientific and Technological Research Council of Turkey (TÜBİTAK), Program BİDEB 2232 (Proje No: 115C010).

6. REFERENCES

1. Szwedzicki, T., 2003. Rock Mass Behaviour Prior to Failure. *Int. J. Rock Mech. Min. Sci.*; 40: 573-584.
2. Rosmanith, H.P., 1983. Modelling of Fracture Process Zones and Singularity Dominated Zones. *Eng. Fract. Mech.*, 17(6), 509–525.
3. Whittaker, B.N., Singh, R.N., Sun, G., 1992. *Rock Fracture Mechanics-Principles, Design and Applications*. Amsterdam: Elsevier, p. 181- 190.
4. Atkinson, C., Smelser, R.E., Sanchez, J., 1982. Combined Mode Fracture Via the Cracked Brazilian Disk Test. *International Journal of Fracture*, 18 (4), p. 279–291.
5. Shetty, D.K., Rosenfield, A.R., Duckworth, W.H., 1985. Fracture Toughness of Ceramics Measured by a Chevron Notch Diametral Compression Test. *Journal of American Ceramics Society*, 68 (12), p. C325–C327.
6. Swartz, S.E., Taha, N.M., 1990. Mixed Mode Crack Propagation and Fracture in Concrete. *Engineering Fracture Mechanics* 35, p. 137–144.
7. Larsson, S.G., Carlsson, A.J., 1973. Influence of Non-singular Stress Terms and Specimen Geometry on Small Scale Yielding at Crack Tips in Elastoplastic Materials. *Journal of the Mechanics and Physics of Solids*, 21, p. 263–277.
8. Lawn, B.R., 1993. *Fracture of Brittle Solids*. Cambridge University Press. Cambridge.
9. Erarslan, N., Williams D.J., 2013. Mixed Mode Fracturing of Rocks under Static and Cyclic Loading, *Rock Mechanics and Rock Engineering*, 46, (5), p. 1035–1052.
10. Ghamgosar M., 2017. PhD Thesis. Micromechanical and Microstructural Aspects Affecting Rock Damage, Fracture and Cutting Mechanisms. The University of Queensland, Australia.
11. Irwin, G.R., 1948. *Fracture Dynamics*. Fracture of Metals, American Society of Metals, p. 147–166.
12. Hoek, E., Bieniawski, Z.T., 1965. Brittle Fracture Propagation in Rock under Compression. *International Journal of Fracture Mechanics*, 1, p. 137–155.
13. Al-Shayea, N.A., 2005. Crack Propagation Trajectories for Rocks under Mixed Mode I–II Fracture, *Engineering Geology*, 81, p. 84–97.
14. Li, Y.P., Chen, L.Z., Wang, Y.H., 2005. Experimental Research on Pre-cracked Marble under Compression. *International Journal of Solids and Structures*, 42, p. 2505–2516.
15. Erdogan, F., Sih, G.C., 1976. On the Crack Extension in Plates under Plane Loading and Transverse Shear, *ASME Journal of Basic Engineering*, 10, p. 25–37 .
16. Awaji, H., Sato, S., 1978. Combined Mode Fracture Toughness Measurement by the Disk Test. *Journal of Engineering Materials Technology*, 100, p. 175–182.
17. Smith, D.J., Ayatollahi, M. R., Pavier, M.J., 2001. The Role of T-stress in Brittle Fracture for Linear Elastic Materials under Mixed Mode Loading. *Fatigue and Fracture of Engineering Materials and Structures* 24(2), p. 137–150.
18. Al-Maghrabi, M.N.N., Abd-Elhady, A.A., 2013. Effective Stress Intensity Factor of Rock-like Brittle Materials Subjected to Different Mode of Mixity. *Journal of American Science*, 9(3), p. 216-220.

19. Wawrzynek, P., Ingraffea, A., 1987. Interactive Finite Element Analysis of Fracture Processes: An Integrated Approach. *Theoretical and Applied Fracture Mechanics*, 8: p. 137-150.
20. ISRM, 1978. International Society for Rock Mechanics. Suggested Methods for Determining Tensile Strength of Rock Materials. *International Journal of Rock Mechanics, Mining Science and Geomechanics Abstracts*, 15, p. 99–103.

